Pattern selection induced by electroconvection in the electrodeposition of iron

Ke-Qin Zhang, Mu Wang,* Sheng Zhong, Guo-Xin Chen, and Nai-ben Ming
National Laboratory of Solid State Microstructures and Department of Physics, Nanjing University, Nanjing 210093, China
(Received 2 July 1999; revised manuscript received 25 October 1999)

The morphology of iron electrodeposit is shown to relate closely to the pH of the electrolyte solution. Macroscopically, depending on the strength of the interbranch convection, which is associated with the concentration of H_3O^+ in the electrolyte, the deposit morphology varies from treelike pattern to meshlike pattern and dense-branching morphology. Microscopically the deposit is ramified and dense-branching at lower concentration of H_3O^+, while it becomes relatively smooth and stringy at higher H_3O^+ concentration. The symmetry of the convective vortices on the two sides of the growing tip is observed to decide the growth behavior of the tip. We suggest that H_3O^+ influences the pattern formation and pattern selection in the electrodeposition of iron from $FeSO_4$ solution by either initiating interbranch convection or changing the effective interfacial energy of the deposit and the electrolyte.

PACS number(s): 81.15.Pq, 47.54.+r, 47.20.Hw, 92.60.Ek

I. INTRODUCTION

The mechanism of pattern formation and pattern selection is an important aspect of nonequilibrium interfacial growth [1–4]. Electrodeposition of metal from a thin electrolyte film is frequently used to study ramified growth. Yet the behind mechanism is much more complicated than the original expectations [5]. Different morphological phase diagrams in the electrodeposition of zinc sulfate were found with similar experimental design and control parameters [6,7]. Later experiments using copper electrodes and parallel geometry generated more dissimilar results [8]. So it is a desire for a long time in electrodeposition to capture the essential physics governing the pattern formation and pattern selection. Fleury and his coworkers studied the hydrodynamics of the electrolyte solution near the growing tips [9]. A coulombic force was claimed to act on the fluid nearby the deposit tips in their model and the growth speed of the deposit matched the speed at which the anions withdraw from the deposit. Meanwhile two vortices between the neighboring tips of the deposit branches were expected. The largest loops of the vortices formed an arch which separated two regions: a depleted region (the area below the arch) and a region with constant concentration (above the arch). By interference contrast microscopy or phase contrast microscopy, the concentration gradient across the arch can be outlined. It has been demonstrated that the interbranch convection affects pattern formation significantly. For example, in the case of strong interbranch electroconvection the neighboring tips approached each other along the arch to form closed loops [10]. When the interbranch convection became less evident, the deposit morphology changed back to the dense-branching morphology. Actually formation of loops driven by electroconvection was not restricted to the electrodeposition of $FeSO_4$. It can be observed in other electrodeposition systems as well [11]. In addition to the electroconvection, other physical and chemical factors also affect the growth morphology in electrochemical deposition [12–14]. Up to now several dynamic morphological transitions have been reported in the quasi-two-dimensional electrodeposition [15–21]. One type of morphological transition is characterized by a sudden change of the branching rate and/or color of the deposit, which has been suggested to result from the interaction of the growing deposit with the chemical fronts advancing from the anode towards the cathode [15–18]. This kind of transition was also claimed to relate to the exhaustion of metal ions in the electrolyte [19]. Another type of morphological transition occurs alternately between two morphologies on each deposit branch independently, which is assumed to result from a local oscillatory H_3O^+ concentration in front of the growing interface [20]. We are convinced that the investigation of the local physical/chemical environment is essential to understand the mechanism of pattern formation and pattern selection.

In this paper, we present our studies on the morphological transitions in the electrochemical deposition of $FeSO_4$. With the help of interference contrast microscopy, we demonstrate how the interbranch convection selects the growth of a specific deposit branch. We also discuss the relation of the local concentration of H_3O^+ and the initiation of interbranch electroconvection; the stability of the concentration field in relation to the pH of the electrolyte, as well as the reappearance of a specific deposit morphology that dominated the deposition before the morphology transition took place.

II. EXPERIMENT

The electrochemical deposition of $FeSO_4$ was carried out in the electrolyte sandwiched by two glass plates. Two straight, parallel electrodes were used [10,20]. The anode was made of an iron wire 0.5 mm in diameter (99.99% pure, Goodfellow, UK). The cathode was a graphite rod of the same diameter. The upper glass plate was narrower than the separation of the two electrodes, in this way the separation of the upper and the lower glass plates could be adjusted independent of the thickness of the electrodes, as shown in Fig. 1. It is important that two openings exist between the upper glass plate and the two electrodes, respectively. Otherwise

*Author to whom correspondence should be addressed. Electronic address: muwang@netra.nju.edu.cn

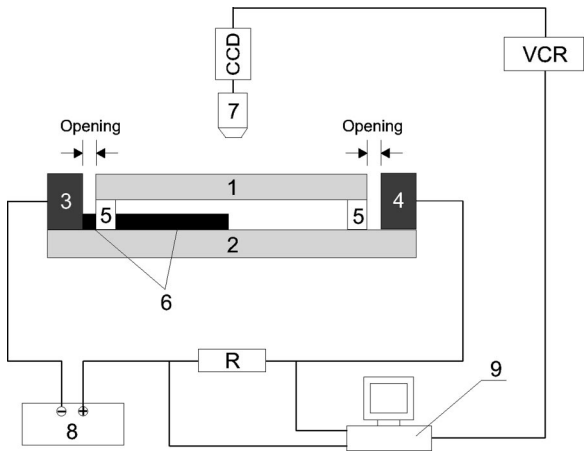

FIG. 1. The schematic diagram to show the experimental setup. (1) Upper glass plate made of microscope slide; (2) lower glass plate made of microscope slide; (3) cathode; (4) anode; (5) spacers made of mica sheet, 30 μm in thickness; (6) metal deposit grown from the cathode; (7) microscope with video system attached to it; (8) power supplier; (9) data acquisition and image processing system.

the hydrogen bubbles generated near the cathode in the early stage of electrodeposition will not be evacuated and will block the growing branches. The thickness of the electrolyte solution was controlled by the mica spacers (30 μm in our experiments). After confirming that both constant-voltage and constant-current experiments generated similar morphologies, we used constant-voltage method in most cases, except in the measurement of deposit growth rate during the morphological transitions. A research optical microscope (Leitz, Orthoplan-pol) with reflection interference contrast device and charge-coupled device video system was used to visualize the concentration gradient in front of the growing interface and to monitor the metal deposition. Analytical grade reagent $FeSO_4$ and deionized water were used to prepare the electrolyte for the experiments. The pH of the electrolyte was measured by a pH meter accurate to ± 0.01. The concentration of $FeSO_4$ solution was 0.5 M and original pH of the electrolyte was 3.72. Dilute sulfuric acid solution could be introduced to $FeSO_4$ electrolyte in order to adjust the pH of the electrolyte. The experiments were carried out at room temperature. The constant voltage applied across the electrodes was in the range of 4.0 and 15.0 V.

III. EXPERIMENTAL RESULTS AND DISCUSSION

When a constant voltage is applied across the electrodes, branches of iron deposit emerge from the cathode. For the acidified $FeSO_4$ electrolyte solution ($pH=2.00$), the initial morphology of the deposit is meshlike. By interference contrast microscopy, dark (or bright) arches connecting the neighboring branches can be visualized, which characterize the presence of interbranch electroconvection, as shown in Fig. 2(a). The tips of the neighboring branches approach each other along the arch and finally form a nearly closed loop, as indicated by two groups of white arrows 1 and 2 in Fig. 2, respectively. Once a loop is formed, the arch in front of the tips disappears. The new branches are generated by bifurcation of the tips, while many tips are terminated by turning to the neighboring one and forming loops. Therefore the total number of the growing tips does not vary significantly during the formation of meshlike pattern. Our observation indicates that the development of the deposit tip depends on the strength of electroconvection on the two sides of the tip. More specifically, tip splitting takes place when the contrast and the shape of the arches on the two sides of the tip are symmetric, as indicated by the dark arrows in Figs. 2(b)–2(c). If the contrast on the two sides of a tip is apparently asymmetric, the tip will ultimately turn to the neighboring branch and form a loop, as that shown inside the white dash-line frame in Figs. 2(c)–2(f). Figure 2 provides the evidence that the interbranch electroconvection influences pattern formation by selecting a specific branch during the growth. Inside the white frame in Fig. 2(c), two arches with different contrast connect three tips. As the deposit grows, one arch takes over the other one and the two arches merge into one arch [Figs. 2(e)–2(f), inside the white frame]. At the same time, the tip in the middle is no longer connected by any arch, and it stops growing soon, as that indicated by the open arrows inside the dash-line frame of Figs. 2(e)–2(f). According to the theory of Fleury *et al.* [9], there should be two vortices under each arch. So inside the white dash-line frame of Fig. 2(c) there exist four vortices under the two arches. When the branch in the middle turns to the left, only one arch remains [Fig. 2(f), inside the white frame], suggesting that only two vortices survive. We suggest that the symmetry and the strength of the convective vortices on the two sides of the growing tips decide the growth behavior of the metal branches.

It has been shown that sufficiently high concentration of H_3O^+ is required to initiate observable interbranch electroconvection [10]. If the electrolyte of $FeSO_4$ is not intentionally acidified (meanwhile $pH\sim 3.72$), the deposit is usually dense-branching, as that illustrated in Fig. 3(a), see also Refs. [10] and [20]. During the growth of dense-branching morphology (DBM), drops of diluted sulfuric acid (pH ~ 1.80) are introduced in front of the growing interface via a small hole on the upper glass plate with a microsyringe. It follows that the deposit morphology changes from DBM to a meshlike pattern accordingly, and the characteristic arches of electroconvection can be recognized, as shown in Figs. 3(b)–3(c). During the development of meshlike pattern in the locally acidified electrolyte, hydrogen bubbles are usually generated in the vicinity of meshlike deposit. Consequently H_3O^+ concentration at the growing front is decreased gradually. When the local concentration of H_3O^+ becomes sufficiently low, either by generating H_2 bubbles or by volume diffusion in the growth cell, the deposit morphology changes back to DBM, as illustrated in Fig. 3(d). This observation confirms that higher concentration of H_3O^+ may initiate interbranch electroconvection and contribute to the formation of meshlike pattern.

The model of Fleury *et al.* [9] implies that any charge accumulation around the deposit tips may induce interbranch convection, and hence affect the pattern formation process. Our recent results indicate that in the electrodeposition of $FeSO_4$ solution the role of H_3O^+ cannot be replaced, at least, by Na^+ and K^+. We add several drops of Na_2SO_4 solution into the system through the small hole on the upper glass plate when the dense-branching deposit approaches. The

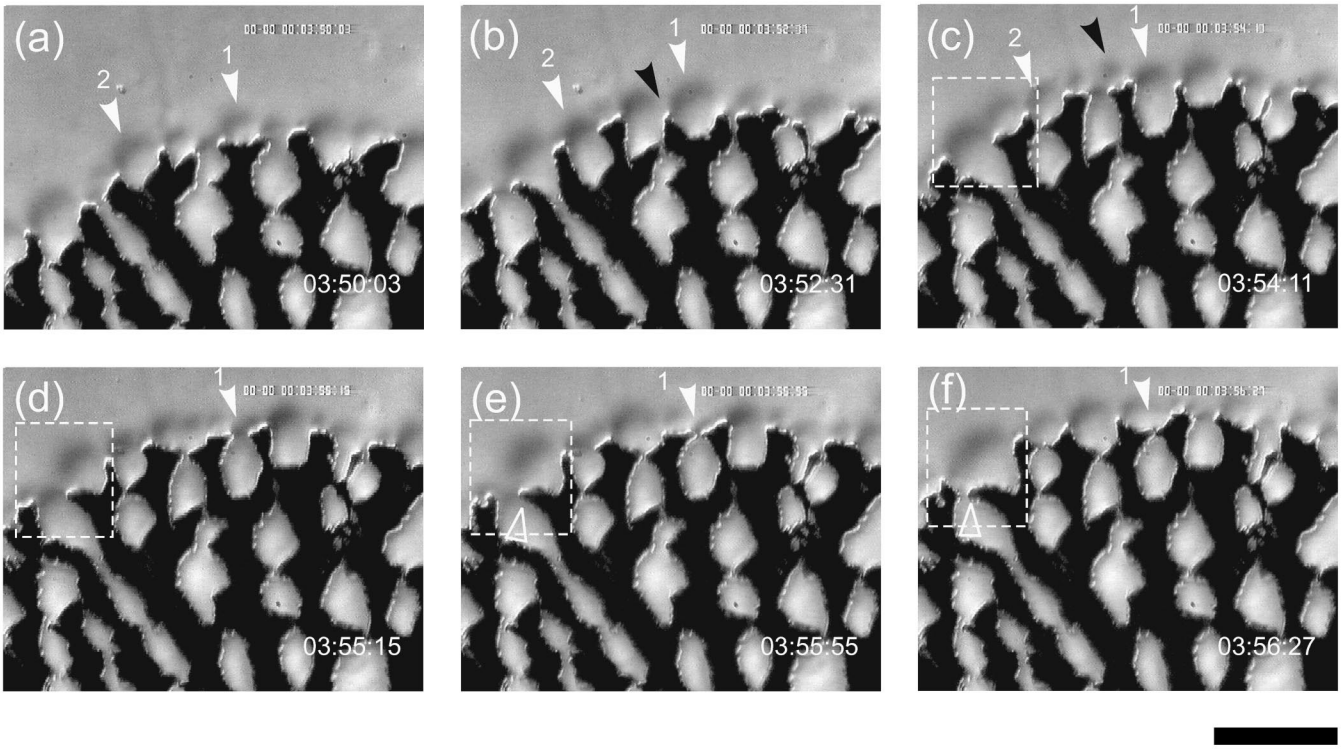

FIG. 2. Formation process of the meshlike pattern during the electrodeposition of iron from $FeSO_4$ aqueous solution (pH=2.00), observed by interference contrast microscopy. The dark arches connecting the neighboring branches characterize the electroconvection between the neighboring branches. The neighboring tips approach each other along the arch and finally form a loop, as indicated by the white arrows 1 and 2, respectively. Bifurcation of the tip can be observed in the growth, which sustains the mesh-forming process. Many tips are terminated when they turn to the neighboring ones to form loops. Whether the tip turns to left or right in the formation of a loop depends on the electroconvection on the two sides of the tip. If the contrast and the shape of the arch, which reflect the strength of the electroconvection, are almost the same on the two sides of the tip, tip spliting usually occurs, as indicated by the dark arrows in (b) and (c). Otherwise the tip will turn to right or left side to form a loop, as shown by the open arrows inside the white dash-line frame in (e) and (f). The voltage across the two parallel, straight electrodes is 6.0 V. The digits at the right-bottom corner are the time scale, representing minute, second, and 1/100 second, respectively. The bar represents 100 μm.

concentration of Na_2SO_4 varies from 0.01 to 0.25 M. We do not observe the characteristic arches of electroconvection and the change of deposit morphology. Instead, the deposit branches stop growing when the solution of Na_2SO_4 is introduced and many precipitate particles emerge in front of the branches. Very often gas bubbles are generated in this process. The situation remains the same when the constant voltage across the electrodes is stepped from 3.0 to 12.0 V with an increase of 1.0 V for each run. Potassium sulfate gives a similar result. Actually the electrodeposition of copper with sodium sulfate as supporting electrolyte has been reported, where hydrogel of copper hydroxide is observed during the deposition [22]. It has been pointed out that in the electrodeposition of copper, alkali metal sulfates in general form copper hydroxide at the copper electrodes [23], which may hinder the further development of the deposit. We suggest that similar situation occurs to the experiments described above. The precipitates that we observed in the electrodeposition of iron are most probably the iron hydroxide.

When the acidified $FeSO_4$ solution (pH=2.00) is used for the electrodeposition, meshlike pattern dominates in the early stage. However, when the meshlike pattern grows for some time, a morphological change from meshlike pattern to DBM has been observed, as shown in Figs. 4(a)–4(d). This transition is attributed to the decreasing of H_3O^+ concentration in the electrolyte solution [10]. It should be noted that the transition shown in Fig. 4 is a gradual process, during which there exist some transient morphologies [Figs. 4(b) and 4(c), for example]. This is different from those reported previously [15–19] that the change of the morphology takes place abruptly over all growing front. Most interestingly, the mesh→DBM evolution can be followed by at least two morphological transitions. When the iron deposit grows in DBM for a sufficiently long time, the deposit morphology changes back to meshlike pattern. As illustrated in Fig. 5(a), the meshlike pattern appears on the growing front simultaneously (also abruptly), together with the characterizing arches representing the interbranch electroconvection in front of the growing tips. When the meshlike pattern grows for a short period, the density of the deposit branches increases suddenly and a very compact growth front appears [Fig. 5(b)]. Thereafter, as illustrated in Fig. 5(c), a treelike, rarefactive branching morphology emerges from the compact deposit. The density of the branches of the treelike pattern is even lower than that of meshlike pattern. In addition, comparing to the typical DBM, the treelike pattern is more stringy. The morphological transitions shown in Fig. 5 are usually observed when the deposit becomes longer than the half of the separation of the electrodes. These morphological changes in Fig. 5 differ from that in Fig. 4 by taking place

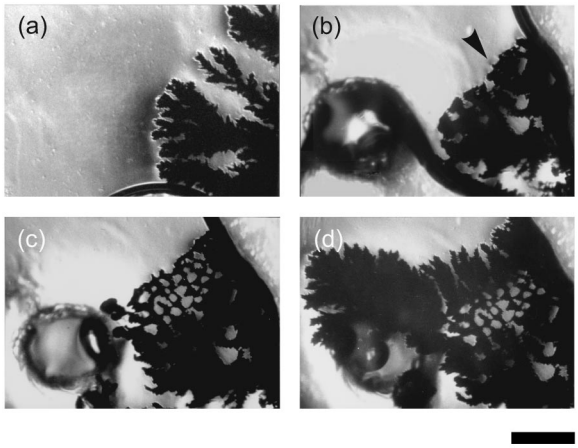

FIG. 3. The evidence to show the role of H_3O^+ in the formation of meshlike pattern. Non-acidified electrolyte is used initially and the deposit morphology is DBM, as shown in (a). A small hole of 0.2 mm in diameter is made on the upper glass plate, where drops of diluted H_2SO_4 (pH=1.80) are introduced when the branches of DBM approach. As the result, the deposit morphology changes from DBM to meshlike pattern, as illustrated in (b) and (c). As indicated by the arrow in Fig. 2(b) the arches connecting the neighboring tips of the deposit can be identified. When the meshlike pattern grows for some time, during which many H_2 bubbles are generated, the deposit morphology changes back to DBM, as shown in (d). The electric voltage across the electrodes is kept 6.0 V during the whole process. The bar represents 200 μm.

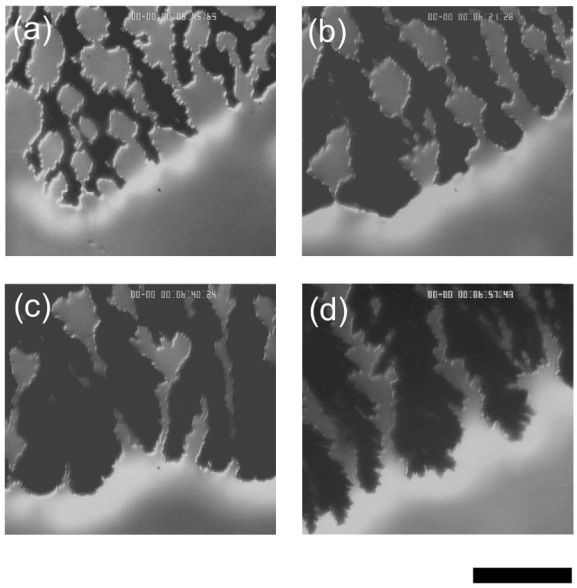

FIG. 4. In acidified $FeSO_4$ solution the initial morphology of the electrodeposit is meshlike, as shown in (a). When the meshlike pattern grows for a while, the branches are thickened and ramified, the deposit morphology changes gradually to dense-branching morphology [(b)–(d)]. This transition takes about 80 seconds, and is expected to relate to the decreasing of H_3O^+ concentration at the growing front. The last three digits in the time scale represent minutes, second, and 1/100 second, respectively. The bar represents 100 μm.

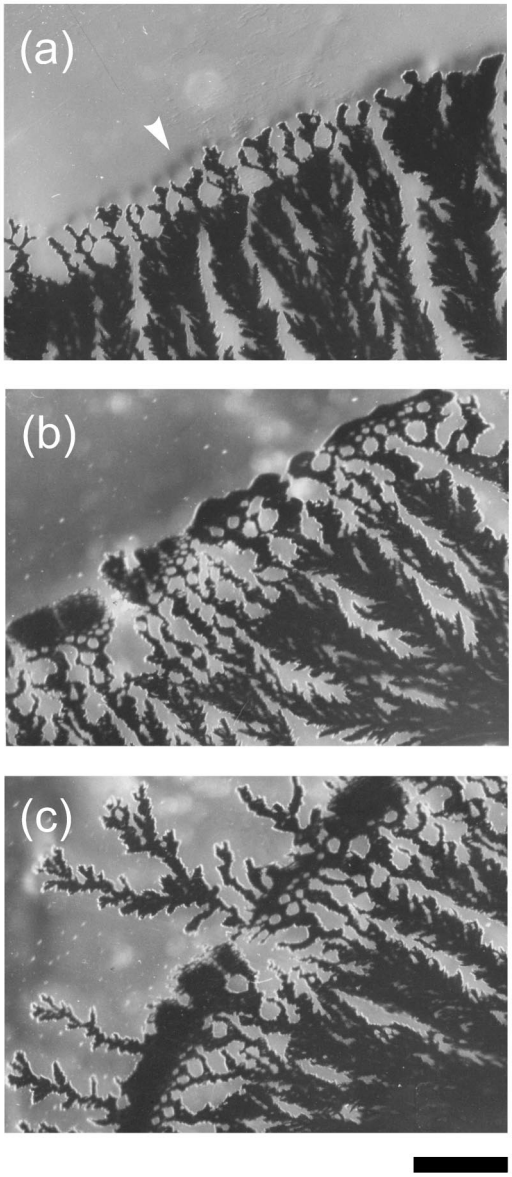

FIG. 5. The morphological transitions take place when the deposits are close to the anode. A sharp transition from DBM to meshlike pattern can be seen in (a), where arches connecting the neighboring branch tips can be recognized, as indicated by the arrow in (a). When the meshlike pattern grows for some time, the growth rate decreases and a compact pattern with higher density appears on the growing front (b). Finally a treelike deposit emerges from the compact front, as shown in (c). The voltage across the electrodes is kept at 12.0 V. The bar represents 200 μm.

abruptly over the growing front.

The concentration profile in front of the growing tips of the treelike deposit varies rapidly both in time and in space. As illustrated by the arrows in Figs. 6(a)–6(b), the contrast in front of the growing tips varies significantly in about one second. The center of the white region in Fig. 6(c), which is marked by the star, shifts to the lower-right corner at a speed of about 33 μm/s. The contrast in front of the growing branches changes chaotically. To quantitatively characterize the dynamic behavior of the concentration field in front of the growing treelike deposit, we select an area of 25×25 pixels and about 4.0 μm away from the growing tip [Fig.

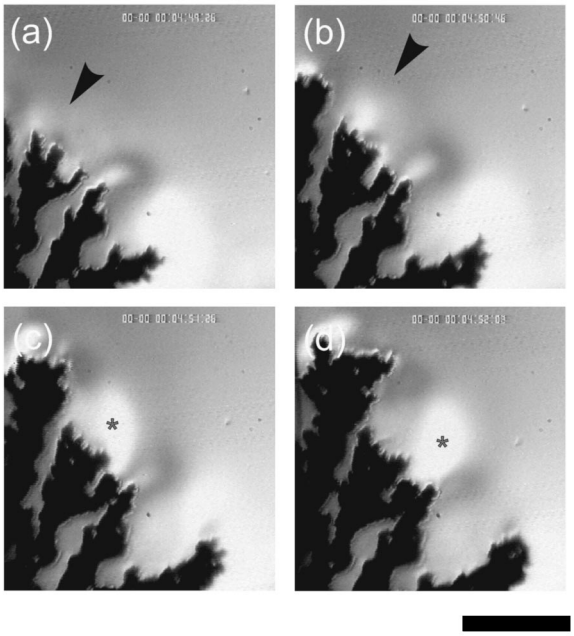

FIG. 6. The unstable concentration profile in front of the growing tips of the treelike deposits. As indicated by the arrows in (a)-(b), the contrast in front of the tips changes significantly in about one second. About one second later, the center of the white region in (c), marked by the star, shifts to the lower-right corner at a speed of about 33 μm/s. The bar represents 100 μm.

7(a)], and measure the average intensity inside this area as a function of time. This is done by an image acquisition and processing system. The contrast is scaled to 0–255. The result is shown in Fig. 7(a). For comparison, we apply the same method to the concentration profile during the growth of DBM [Fig. 7(b)]. As illustrated in Fig. 7(b), a much stable concentration distribution moves steadily as the tips of the deposit grow forward.

To investigate the evolution of the concentration of H_3O^+ adjacent the growing interface during the morphological transition, we measure the pH of the electrolyte as a function of time by very narrow slices of indicator paper. As illustrated in Fig. 8(a), the average pH value increases first and reaches a maximum. Then it decreases continuously. Corresponding to the change of pH value, the deposit morphology transits from meshlike to DBM, and then changes back to a meshlike pattern. In the scenario of sufficiently low pH, a treelike pattern can be observed. The initial increasing of pH value shown in Fig. 8(a) possibly results from the generation of H_2 bubbles during the electrodeposition, which consumes H_3O^+. To find out the explanation for the subsequent decreasing of pH value in the electrolyte, we measure the pH in the vicinity of the anode as a function of time [Fig. 8(b)]. It turns out that the pH near the anode decreases monotonically. So H_3O^+ is indeed generated at the anode, probably due to the hydrolysis of metal ions during the anode dissolution. We suggest that the diffusion of acid front is responsible for the later decreasing of pH shown in Fig. 8(a), and consequently the morphological transitions shown in Fig. 5. The decreasing rate of the pH value at the anode depends on the voltage applied to the electrodes. The high voltage makes the pH drop more rapidly.

The electric current during the electrodeposition process has been measured as a function of time (constant-voltage experiment), as shown in Fig. 9. Since acidified electrolyte solution is used, the morphology of the electrodeposit is meshlike in the early stage. Small fluctuation of electric current has been detected, which is illustrated by the insert on the up-left corner. The duration for the growth of meshlike pattern and the amplitude of the electric current fluctuation

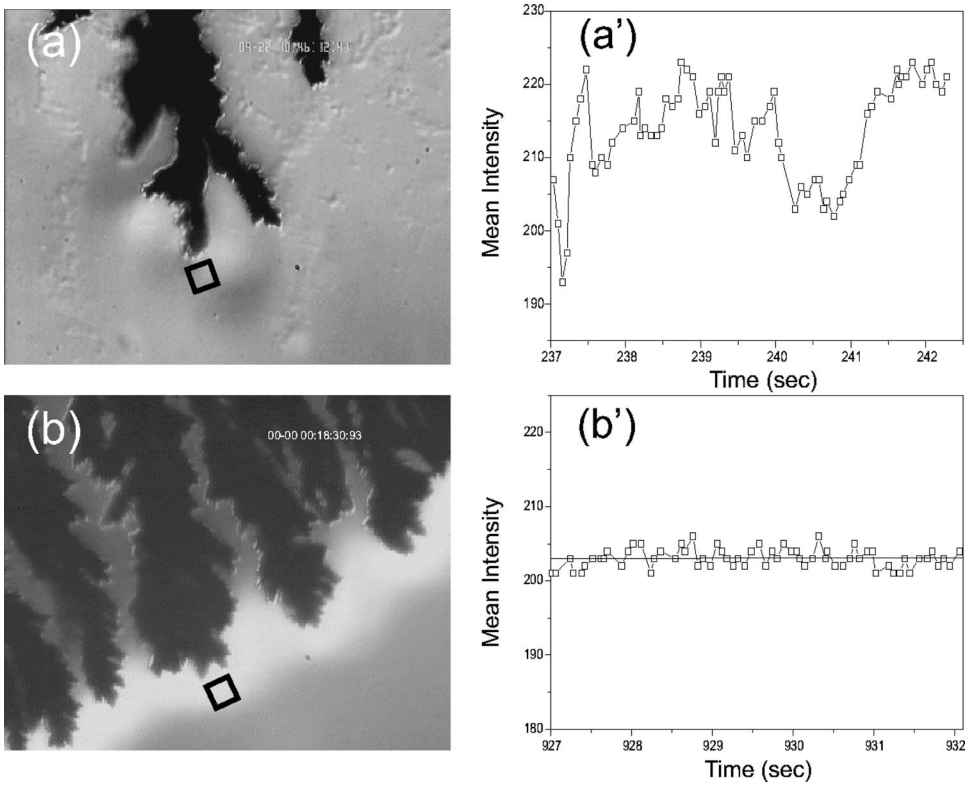

FIG. 7. (a) The chaotically changing concentration field during the growth of treelike iron deposit. To characterize the changing of the concentration field in front of the tips, the intensity inside of an area of fixed size, as that indicated by the black box, is measured as a function of time. The results are shown in (a). The box is kept about 4 μm in front of the tip. (b) For comparison, the dynamic behavior of the concentration field during the growth of DBM is measured. The method is the same as that for the treelike deposit. The intensity inside the box as a function of time is shown in (b), which is much more stable than that in (a).

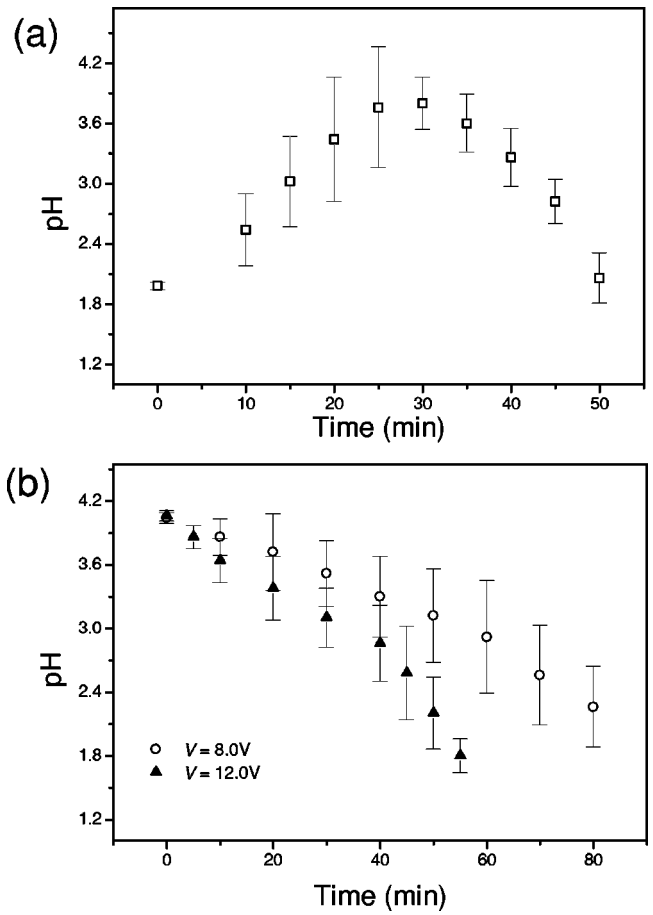

FIG. 8. (a) The average pH value of the electrolyte in front of the deposit measured by very narrow slices of indicator paper (accurate to ± 0.2). The data are collected at different sites between two parallel electrodes along the edge of the cell. These sites are very close to the growing branches. The acidified electrolyte solution is used for the experiment. (b) The pH value of the electrolyte near the anode measured at different applied voltage. The electrolyte is not acidified initially. When electrodeposition proceeds, the pH near the anode gradually decreases and the decreasing rate depends on the applied voltage, indicating that acid front is indeed generated at the anode during the electrodeposition.

depend on the initial concentration of H_3O^+. In the case of lower initial pH of the electrolyte, the meshlike pattern grows longer and the fluctuation of electric current is more significant. For the growth of DBM, the electric current increases steadily, which corresponds to the gradually increasing number of growing tips. While for the growth of the subsequent meshlike pattern and treelike pattern, strong fluctuation of electric current is recorded, as illustrated by the insert on the lower-right corner of Fig. 9. At present time we are not able to distinguish the electric current fluctuation caused by the growth of the re-entrant meshlike pattern and that due to the growth of the treelike pattern. In addition, H_2 bubbles in the electrodeposition also disturb the electric current.

The pH of the electrolyte in relation to the deposit morphology has been investigated quantitatively. The experiments are conducted with the same $FeSO_4$ concentration, but different initial pH of the electrolyte. The voltage applied to the electrodes is fixed at 10.0 V in these measurements and

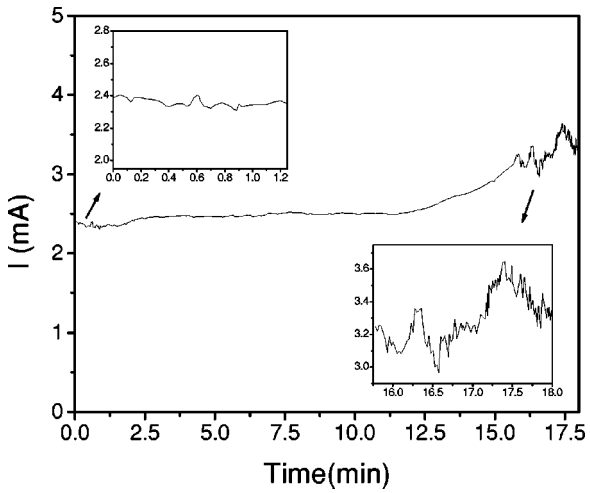

FIG. 9. The typical electric current measured during the electrodeposition from an acidified solution. In the initial stage the deposit is meshlike, and small fluctuation of electric current can be detected, as illustrated by the insert on the left-up corner. As the deposit grows, the morphology changes gradually to DBM. During the growth of DBM the electric current is relatively stable, and increases gradually. When the deposit grows for some time, the deposit becomes meshlike, and subsequently treelike, whereupon strong fluctuation of electric current can be seen (right-down corner).

the deposit morphologies we mentioned in this paragraph are the morphologies observed in the early stage of electrodeposition. It turns out that when the average pH of the electrolyte is below 2.00, the deposit is usually treelike and the concentration profile in front of the deposit branches fluctuates significantly both in time and in space, as that shown in Figs. 6 and 7(a), respectively. When pH of the electrolyte is in the range of 2.00 and 2.22, the deposit branches approach each other and a meshlike pattern is formed. When the pH value becomes higher than 2.22, the deposit turns to DBM. The boundaries in this morphological ''phase diagram'' are not very sharp. The deviation of pH corresponding to the dispersed boundary can be as high as 0.10.

The average interfacial growth rate of the electrodeposit in the same run is also measured as a function of time when the initial pH of the electrolyte is about 1.80, the result is shown in Fig. 10. For this measurement a galvanostatic power supply is used and the electric current is fixed at 4.0 mA. This means that the mass deposition rate is kept constant. Due to the low initial pH of the electrolyte, in the early stage the deposit branch is treelike. The typical growth rate is above 15 μm/s. During this process the average growth rate is decreasing because the number of the growing tips is increasing. As the deposit develops, an evolution from treelike pattern to meshlike pattern occurs. During the growth of meshlike pattern, the average deposit growth rate does not change significantly, meaning that the number of the growing tips does not increase significantly, which is consistent with our optical observations. As time goes on, a transition from meshlike pattern to DBM is observed. The growth rate for DBM drops gradually, because tip splitting is an important feature of DBM growth, and more growing tips decelerate the average moving speed of the growth front.

As an example of morphological transition in elec-

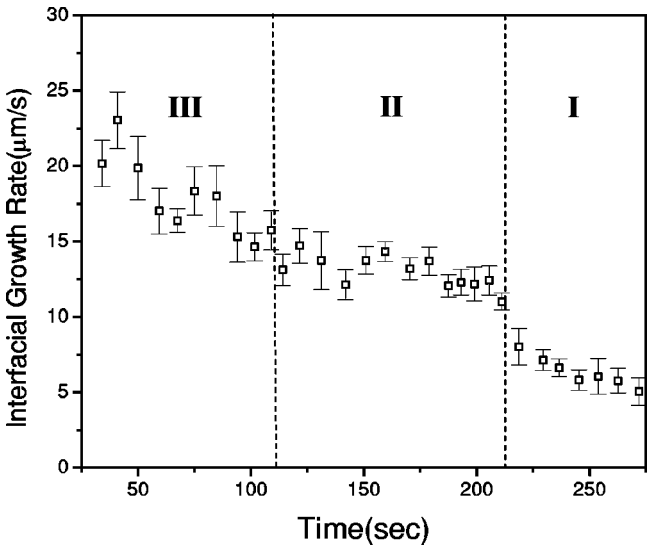

FIG. 10. The average interfacial growth rate of the electrodeposit measured as a function of time. Meanwhile galvanostatic power supplier is used and the electric current is fixed at 4.0 mA. The initial pH of the solution is 1.80. In the regions I, II, and III, the deposits are dense-branching, meshlike, and treelike, respectively.

trodeposition, Hecker transition has been investigated by several groups [15–19,21]. This effect is generally described as a sudden change of branch density and/or color, growth rate, etc., of the deposit. The location of the morphology transition has been reported to scale with the electrodes separation in some systems. It is generally believed that this transition is associated with different chemical fronts encountered by the deposit branch [15,16]. Our experimental observations support the idea that the morphological transition in electrodeposition is associated with the change of the concentration of H_3O^+ in front of the growing interface. If the change of H_3O^+ concentration is due to the generation of H_2 bubbles, the variation of chemical contents will be a gradual process. Therefore, the evolution of deposit morphology as that shown in Fig. 4 will be observed. If, however, the change of H_3O^+ concentration in front of the growing interface is due to the encounter of chemical front coming from the anode, a sudden change of deposit morphology as that shown in Fig. 5 will be observed.

Microscopic morphology of the deposit provides the information of local growth environment and possibly the interfacial growth mechanism. High resolution microscopy indicates that the DBM actually consists of many tiny dendrites [20,24]. The tips of these tiny dendrites frequently split during the growth. When the concentration of H_3O^+ becomes sufficiently high, the branching rate of the deposit decreases considerably and the surface of the branches becomes much more compact than that of DBM [24]. Concerning the behind mechanism, one possibility is that the high concentration of H_3O^+ modifies the interfacial energy of the iron deposit and the electrolyte, and hence modulates the microscopic morphology of the electrodeposit. As the matter of fact, the interfacial energy depends on the interactions of the atoms, ions and molecules on the two sides of the growth front [25], and is sensitive to the change of the chemical and physical conditions at the interface. Computer simulations have demonstrated that by introducing the effect of surface tension in the diffusion-limited growth, the interfacial morphology may vary from a ramified, fractal-like pattern to a compact, fingering pattern [26,27]. It is true that the presence of H_3O^+ changes the chemical environment of interfacial growth and the oxidation on the deposit surface. Such scenario has been reported in the electrodeposition of copper [28]. Our recent Mössbauer spectroscopy study of the deposits, however, shows that the valent of iron in the deposit is not changed corresponding to the variation of the deposit morphology [24]. On the macroscopic scale, interbranch electroconvection affects the deposit morphology when the convection is strong. Since the electroconvection is sensitive to the concentration of H_3O^+, while H_3O^+ always exists in aqueous electrolyte solution, in this sense, electroconvection is indeed a common ingredient affecting the pattern formation in electrochemical deposition.

IV. CONCLUSIONS

We demonstrate in this paper that the morphology of the iron electrodeposit is closely related to the interbranch electroconvection, while the electroconvection relies on the local concentration of H_3O^+ at the growing front. With the help of interference contrast microscopy, we show how the interbranch convection contributes to the selection of a specific deposit branch during the growth. On the macroscopic scale the deposit morphology varies from treelike pattern to meshlike pattern and dense branch morphology depending on the strength of interbranch electroconvection. Microscopically the deposit changes from a ramified, dense branched morphology at lower concentration of H_3O^+ to a more stringy and treelike morphology at higher H_3O^+ concentration. We suggest that the concentration of H_3O^+ influences the pattern formation and pattern selection in the electrodeposition of $FeSO_4$ solution by either initiating interbranch convection or changing the effective interfacial energy of the deposit.

ACKNOWLEDGMENTS

The support by the State Key Program for Basic Research from the Ministry of Science and Technology of China and by the Natural Science Foundation of China are acknowledged.

[1] T. Vicsek, *Fractal Growth Phenomena*, 2nd edition (World Scientific, Singapore, 1992).
[2] R. M. Brady and R. C. Ball, Nature (London) **309**, 225 (1984).
[3] E. Ben-Jacob and P. Garik, Nature (London) **343**, 523 (1990).
[4] T. A. Witten and L. M. Sander, Phys. Rev. Lett. **47**, 1400 (1981); Phys. Rev. B **27**, 1495 (1983).
[5] M. Matsushita, Y. Hayakawa, and Y. Sawada, Phys. Rev. A **32**, 3814 (1985).
[6] Y. Sawada, A. Dougherty, and J. P. Gollub, Phys. Rev. Lett. **56**, 1260 (1986).

[7] D. Grier, E. Ben-Jacob, R. Clarke, and L. M. Sander, Phys. Rev. Lett. **56**, 1264 (1986).
[8] P. P. Trigueros, J. Claret, F. Mas, and F. Sagues, J. Electroanal. Chem. **312**, 219 (1991).
[9] V. Fleury, J.-N. Chazalviel, and M. Rosso, Phys. Rev. Lett. **68**, 2492 (1992); Phys. Rev. E **48**, 1279 (1993).
[10] Mu Wang, Williem J. P. van Enckevort, Nai-ben Ming, and Piet Bennema, Nature (London) **367**, 438 (1994).
[11] Formation of loops can be observed in the electrodeposition of copper from $CuSO_4$ solution, although it is not as evident as what we show in Fig. 2 of this paper. This can be seen in some published papers, for example, V. Fleury, J. H. Haufman, and D. B. Hibbert, Nature (London) **367**, 435 (1994).
[12] D. P. Barkey, D. Watt, Z. Liu, and S. Raber, J. Electrochem. Soc. **141**, 1206 (1994).
[13] J. R. de Bruyn, Phys. Rev. Lett. **74**, 4843 (1995).
[14] J. M. Huth, H. L. Swinney, W. D. McCormick, A. Kuhn, and F. Argoul, Phys. Rev. E **51**, 3444 (1995).
[15] J. R. Melrose, D. B. Hibbert, and R. C. Ball, Phys. Rev. Lett. **65**, 3009 (1990).
[16] V. Fleury, M. Rosso, and J. N. Chazalviel, Phys. Rev. A **43**, 6908 (1991).
[17] M.-Q. Lopez-Salvans, F. Sagues, J. Claret, and J. Bassas, J. Electroanal. Chem. **421**, 205 (1997).
[18] M. A. Guzman, R. D. Freimuth, P. U. Pendse, M. C. Veinott, and L. Lam, in *Nonlinear Structures in Physical Chemistry*, edited by L. Lam and H. C. Morris (Springer, New York, 1990), p. 32.
[19] O. Zik and E. Moses, Phys. Rev. E **53**, 1760 (1996).
[20] Mu Wang and Nai-ben Ming, Phys. Rev. Lett. **71**, 113 (1993).
[21] A. Kuhn and F. Argoul, Phys. Rev. E **49**, 4298 (1994).
[22] S. N. Atchison, R. P. Burford, C. P. Whitby, and D. B. Hibbert, J. Electroanal. Chem. **399**, 71 (1995).
[23] M. Pourbaix, *Atlas of Electrochemical Equilibria in Aqueous Solutions*, (Pergamon Press, Oxford, 1966).
[24] K. Q. Zhang *et al*. (to be published).
[25] X. Y. Liu, J. Chem. Phys. **98**, 8154 (1993).
[26] T. Vicsek, Phys. Rev. Lett. **53**, 2281 (1984).
[27] P. Meakin, F. Family, and T. Vicsek, J. Colloid Interface Sci. **117**, 394 (1987).
[28] M.-Q. Lopez-Salvans, F. Sagues, J. Claret, and J. Bassas, Phys. Rev. E **56**, 6869 (1997).